Simulation of Two-Channel Decay of Excited State in Quantum Register

M. Ostrowski*

Institute of Information Technology FTIMS, Lodz University of Technology, Wólczańska 215, 93-005, Łódź, Poland

Received: 27.05.2022 & Accepted: 29.07.2022

Doi: 10.12693/APhysPolA.142.503 *e-mail: marcin.ostrowski@p.lodz.pl

In this paper, we propose a quantum algorithm simulating the interaction between an atom and a one-dimensional electromagnetic quantum field. We examine the two-channel decay of the atom excited state with the emission of photons. The paper studies the properties of the proposed algorithm and then compares the obtained results with theoretical predictions.

topics: quantum computing, quantum simulations, excited state decay

1. Introduction

In the near future, quantum calculations can make a major contribution to the development of informatics [1]. Nowadays, some institutions claim to have a quantum computer and offer its computing power. Probably wider access to these machines will become possible soon (perhaps with the help of quantum dots technology [2] or using anyons in a topological quantum computer [3]). Therefore, it is worth examining what new possibilities are offered by quantum computing.

For many years, we have known Shor [4] and Grover [5, 6] algorithms which are of lower computational complexity than their best classical counterparts. Another promising application of a quantum computer are quantum simulations [7–9], i.e., computer modeling of physical quantum systems. It gives the possibility of effective modeling quantum processes, which is not possible using classical computers [10]. Quantum computers can simulate a wide variety of quantum systems, including fermionic lattice models [11, 12], quantum chemistry [13, 14], and quantum field theories [15].

As is well known, simulations of quantum systems performed with the use of conventional computers are not effective. This means that for a classical computer, the memory resources and the time required for simulation grow exponentially with the size of the quantum system. In the case of a quantum computer, the situation is different. The relationship between the size of the quantum computer (register) and the size of the simulated quantum system is linear. Therefore, a very important task is to find appropriate algorithms that can properly simulate complex quantum systems and non-trivial interactions between them. This is a difficult issue because most of the interesting quantum systems are feasible in infinitely-dimensional Hilbert spaces. In such situations, we can use the technique of sampling the wave function and build an algorithm based on the quantum Fourier transform. This case was tested in [16–19] where the free Schrödinger particle and the harmonic oscillator were examined. In our previous works, we have shown that also rectangular potentials (like thresholds and wells) can be simulated with this method. This provides the opportunity to examine other interesting processes such as diffusion [20] and scattering [21] of the Schrödinger particle.

Another important issue is the simulation of quantum optics processes, such as the photon emission or absorption by an atom or a molecule. This requires simulating an electromagnetic quantum field, which is a system with an infinite number of degrees of freedom. In this case, we can replace the continuous band of energy levels with its discrete counterpart. We use this method in the current publication as well as in [21, 22]. In the abovementioned works, we successfully simulated the process of atom deexcitation. The disadvantage of the algorithm used is the sparse coding of states in the quantum register (one level per qubit). For this reason, we could only simulate a few photon energy levels. In current considerations, we have proposed a new, more complex algorithm that enables dense coding of photon states in the register. In n_q qubits we can encode 2^{n_q} photon levels. This allows us to store the states of two independent photons in a register of 12–16 qubits. In this work, we use this possibility to simulate the two-channel decay of the atom excited state. Furthermore, we have made a complete redevelopment of the interaction algorithm. Quantum gates have been reordered using the Gray

code sequence. This reduced the number of auxiliary (σ_x and CNOT) gates to a minimum and significantly shortened the computation time.

A theoretical approach to the problem of unstable quantum systems decay can be found in [23]. Works of other authors also focus on simulating the decay of excited states. Models based on cavity quantum electrodynamics (QED) are particularly tested. For example, processes such as beta decay of the helium atom [24] and the decay of a two-level atom in a crystal [25] are examined. Contrary to the cited works, we examine the problem on a purely algorithmic ground, using the abstract model of quantum gates. We completely abstract from specified physical implementation.

In the papers [26–28] quantum computing methods are used in order to find the excited state of a molecule and study its properties. However, the above-mentioned works do not analyse the problem of photon emission. In the paper [29] the optical radiation from a two-level atom is tested numerically (using a damping oscillator description of a dipole current). Unfortunately, in [29] the authors do not propose a quantum algorithm. In the paper [30] an approach similar to ours is investigated. However, only the algorithm for the single photon mode is presented there.

In order to simulate the quantum register, we used a simple environment written in C++ language based on direct matrix multiplication. We also performed several tests of the algorithm with the use of the Qiskit SDK environment [31]. In both cases, we obtained the same results.

2. Description of the simulated system

Let us consider a complex quantum system that is composed of three parts: A, F_1 and F_2 (as shown in Fig. 1). The subsystem A (atom) has two energy levels, i.e., the level $|0\rangle_\mathrm{A}$ with energy equal to zero (the ground state) and the level $|1\rangle_\mathrm{A}$ with the energy E_A (the excited state). We identify the subsystems F_i with photons (without spin) trapped inside a one-dimensional cavity of length $x_{\max}$ (with periodic boundary conditions ($\psi(0) = \psi(x_{\max})$). Additionally, we assume that both photons are mutually distinguishable (they are quanta of two different fields). The base states of each subsystem F_i are denoted by $|n\rangle_{\mathrm{F}_i}$. We identify the state $|0\rangle_{\mathrm{F}_i}$ with the vacuum state (no photon in the cavity). Other states for ($n \neq 0$) are stationary states of a single photon with a wavenumber equal to

$$k_n = n\Delta k \quad \text{for} \quad n = n_{\min}{+}1, n_{\min}{+}2, \ldots, n_{\max}, \tag{1}$$

where $\Delta k = 2\pi/x_{\max}$. Due to the limited capacity of the quantum register, we assume that the energy spectrum of each photon is bounded ($n_{\min} < n \leq n_{\max}$). Only $|n\rangle_{\mathrm{F}_i}$ levels with energy close to E_A are simulated. The probability of filling the remaining levels is negligible.

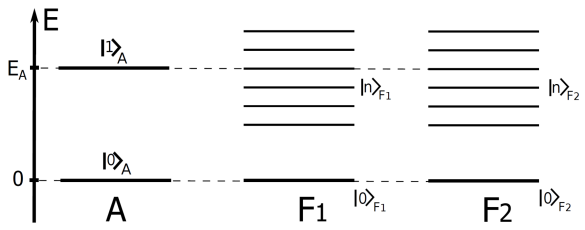

Fig. 1. Scheme of the simulated system. Lower energy levels of photons (with negligibly low occupation probability) are not simulated.

The following operator is chosen as the Hamiltonian of interaction between subsystems A and F_i

$$\hat{H}_{\mathrm{AF}_i} = \sum_{n=n_{\min}+1}^{n_{\max}} \frac{1}{\sqrt{-\omega_n}} \left(g_{in}\hat{a}^\dagger \hat{b}_{in} + g_{in}^* \hat{a}\hat{b}_{in}^\dagger \right), \tag{2}$$

where $\hat{a}$ is the energy decreasing operator of the subsystem A ($\hat{a}|1\rangle_\mathrm{A} = |0\rangle_\mathrm{A}$; $\hat{a}^\dagger|0\rangle_\mathrm{A} = |1\rangle_\mathrm{A}$), $\hat{b}_{in}$ is the annihilation operator of the subsystem F_i ($\hat{b}_{in}|n\rangle_{\mathrm{F}_i} = |0\rangle_{\mathrm{F}_i}$; $\hat{b}_{in}^\dagger|0\rangle_{\mathrm{F}_i} = |n\rangle_{\mathrm{F}_i}$) and $\omega_n = ck_n$. The complex parameters g_{in} are the coupling constants (given in the Appendix by (17)). The Hamiltonian (2) describes transitions between states in the form $|0\rangle_\mathrm{A}|n\rangle_{\mathrm{F}_i} \leftrightarrow |1\rangle_\mathrm{A}|0\rangle_{\mathrm{F}_i}$).

The total Hamiltonian of the system $\mathrm{AF_1F_2}$ has the form

$$\hat{H} = E_\mathrm{A}\hat{a}^\dagger\hat{a} + \sum_{n=n_{\min}+1}^{n_{\max}} E_n \hat{b}_{1n}^\dagger \hat{b}_{1n} + \sum_{n=n_{\min}+1}^{n_{\max}} E_n \hat{b}_{2n}^\dagger \hat{b}_{2n} + \hat{H}_{\mathrm{AF}_1} + \hat{H}_{\mathrm{AF}_2}, \tag{3}$$

where $E_n = c\hbar k_n$.

In order to solve the Schrödinger equation for the Hamiltonian (3), we use the time evolution operator in the form

$$\hat{U}(\mathrm{d}t) = \exp\left[-\mathrm{i}\hat{H}\,\mathrm{d}t/\hbar\right]. \tag{4}$$

For $\mathrm{d}t \to 0$ the operator given by (4) can be approximated as follows

$$\hat{U}(\mathrm{d}t) = \exp\left(-\frac{\mathrm{i}E_\mathrm{A}}{\hbar}\hat{a}^\dagger\hat{a}\,\mathrm{d}t\right) \times \prod_{i=1}^{2}\prod_{n} \exp\left(-\frac{\mathrm{i}E_n}{\hbar}\hat{b}_{in}^\dagger\hat{b}_{in}\,\mathrm{d}t\right) \times \prod_{i=1}^{2}\prod_{n} \exp\left(-\frac{\mathrm{i}}{\hbar}(g_{in}\hat{a}^\dagger\hat{b}_{in} + g_{in}^*\hat{a}\hat{b}_{in}^\dagger)\,\mathrm{d}t\right), \tag{5}$$

where the product over n goes from $n_{\min}{+}1$ to $n_{\max}$. The above equation (5) is equivalent to using the first-order Lie-Trotter formula with Trotter error $\mathcal{O}(t^2)$ [32]. The simulation for a longer time t is obtained by dividing the evolution into n Trotter steps ($t = n\,\mathrm{d}t$).

3. Algorithm simulating the propagation of a free photon

State of each photon is encoded in the momentum representation in the n_f-qubit subregister (subregisters F_1 and F_2). The base states of the F_1 and F_2 subregisters are denoted by $|j\rangle_1$ and $|j\rangle_2$, respectively, where $j = 0, 1, \ldots, 2^{n_f}-1$. Let us consider two possibilities:

- a photon with only positive momentum ($k_n > 0$);
  In this case, the state for j=0 (state $|00\ldots0\rangle$) encodes the vacuum state. Other base states of the subregister — from j=1 (state $|00\ldots01\rangle$) to j=$2^{n_f}-1$ (state $|11\ldots11\rangle$) — encode a photon with the wavenumber $k_{j+n_{\min}}$, i.e., n=j+$n_{\min}$ (see (1)). In this situation, $n_{\max}$=$n_{\min}$+$2^{n_f}-1$.
- a photon with the momentum of any sign;
  In this case, the oldest qubit (n_f-1) encodes the photon momentum sign (state $|0\rangle$ corresponds to $k_j > 0$, while state $|1\rangle$ encodes the case of $k_j < 0$). The rest of the qubits encode $|k_j|$. Both register states $j = 0$ (state $|00..0\rangle$) and $j = 2^{n_f-1}$ (state $|10\ldots0\rangle$) encode the vacuum state (but the latter is not used). In this situation, $n_{\max}$=$n_{\min} + 2^{n_f-1}-1$.

The algorithm simulating the free propagation of a photon (corresponding to the second and the third components in (3)) is shown in Fig. 2. The gates $P_{a\phi}$ are phase-shift gates that operate according to the scheme

$$|0\rangle \to |0\rangle, \qquad |1\rangle \to \exp(-\mathrm{i}a\phi)\,|1\rangle, \tag{6}$$

where $\phi = \mathrm{d}E\,\mathrm{d}t/\hbar$, and $\mathrm{d}E = 2\pi\hbar c/x_{\max}$ is the distance between adjacent energy levels. The gate $P_{\Delta\phi}$ is a controlled phase-shift gate defined as $|0,0,0,0,0\rangle \to \exp(\mathrm{i}\Delta\phi)\,|0,0,0,0,0\rangle$, where $\Delta\phi = n_{\min}\,\mathrm{d}E\,\mathrm{d}t/\hbar$. It implements a shift of the photon spectrum by the $n_{\min}$ value. This is achieved by a decrease of the vacuum energy by $n_{\min}\,\mathrm{d}E$ in relation to other levels.

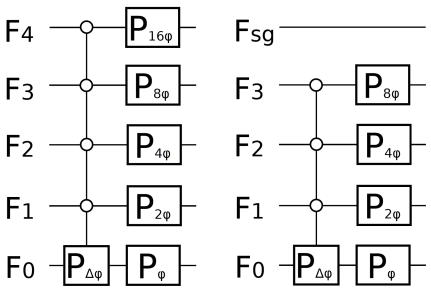

Fig. 2. Algorithms simulating the free propagation of a photon (example for $n_f = 5$). The left scheme shows the algorithm for $k_n > 0$ only, the right one shows the algorithm for k_n of any sign. The oldest qubit (denoted by F_{sg}) encodes the sign of k_n.

4. Algorithm simulating the atom–photon interaction

The scheme of the whole algorithm is shown in Fig. 3. The P_{ϕ_A} gate is a phase shift gate simulating the free evolution of subsystem A (first component in (3)). The phase shift angle for the P_{ϕ_A} gate is equal to $\phi_A = E_A\,\mathrm{d}t/\hbar$. The UF blocks (implementing photon free evolution) were discussed in the previous section (see Fig. 2). The R blocks implement interaction between an atom and a photon.

The implementation of the R block (example for $n_f = 2$) is shown in Fig. 4. Each component of the sum from the Hamiltonian (2) (describing the transition $|0\rangle_A|j+n_{\min}\rangle_{F_i} \leftrightarrow |1\rangle_A|0\rangle_{F_i}$) is simulated by a separate R_j gate which operates as follows

$$|0\rangle \to \cos(\phi_{ij})\,|0\rangle + \mathrm{i}\,\mathrm{e}^{\mathrm{i}\eta_{ij}}\sin(\phi_{ij})\,|1\rangle, \tag{7}$$

$$|1\rangle \to \cos(\phi_{ij})\,|1\rangle + \mathrm{i}\,\mathrm{e}^{-\mathrm{i}\eta_{ij}}\sin(\phi_{ij})\,|0\rangle, \tag{8}$$

where $\phi_{ij} = |g_{i,j+n_{\min}}|\,\mathrm{d}t/\hbar$, $\eta_{ij} = \arg(g_{i,j+n_{\min}})$ and g_{in} are given in the Appendix by (17). The order of the R_j gates follows the Gray code [33] for the j number. As a result, the number of CNOT gates is reduced to a minimum. CNOT gates (with control qubit, active in $|0\rangle$ state) act on a qubit for which a bit flip ($0 \leftrightarrow 1$) occurs in the j number.

The NOT (σ_x) and CNOT gates implement the transformation

$$|0\rangle_A|j\rangle_F \to |0\rangle_A|1\ldots1\rangle_F, \tag{9}$$

$$|1\rangle_A|0\rangle_F \to |1\rangle_A|1\ldots1\rangle_F. \tag{10}$$

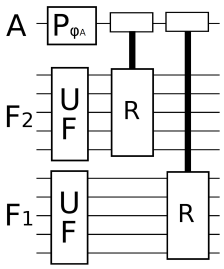

Fig. 3. Scheme of the algorithm. The UF block implements the photon free evolution (Fig. 2). The P_{ϕ_A} gate simulates the free evolution of an atom. The R blocks implement interaction between the atom and the photon. A sample implementation of the R block is shown in Fig. 4.

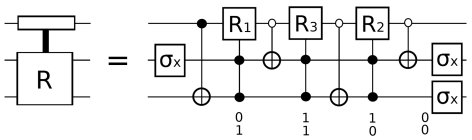

Fig. 4. Implementation of block R (for $n_f = 2$) simulating interaction between an atom (the highest qubit) with a photon. The numbers below the R_j gates are binary representation of the j number.

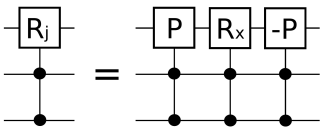

Fig. 5. Implementation of gate R_j (for $n_f = 2$). Gates denoted by P and -P are standard phase shift gates. The phase angle is equal to η_{ij} for the first P gate and $-\eta_{ij}$ for the gate denoted by -P. The R_x gate parameter is equal to $\phi = -2\phi_{ij}$.

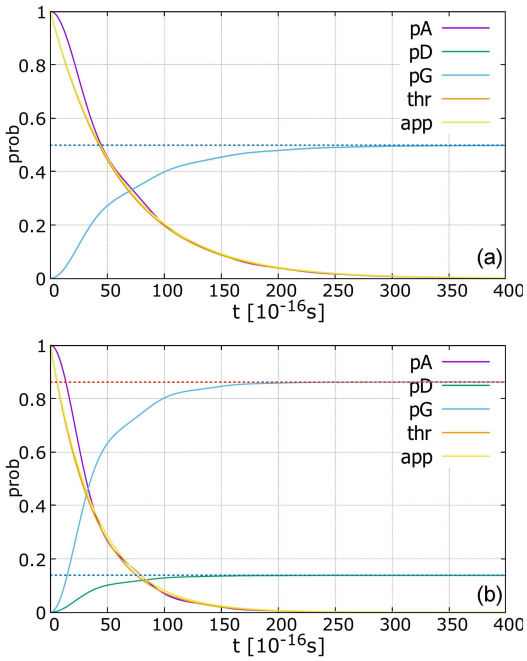

Fig. 6. Excited state decay as a function of time (in 10^{-16} s units). The following curves are shown: pA — probability of finding the atom in the excited state; pD — emission probability of the first photon; pG — emission probability of the second photon; thr — theoretical prediction of pA, app — approximation of pA by an exponential function. The plots are made (a) for $g_{1n} = g_{2n} = 1.6 \times 10^{-13}$ J/$\sqrt{\text{s}}$ and (b) for $g_{1n} = 1.1 \times 10^{-13}$ J/$\sqrt{\text{s}}$ and $g_{2n} = 2.8 \times 10^{-13}$ J/$\sqrt{\text{s}}$. In panel (a), the curve pD is not visible because it overlaps with the pG curve. A similar situation occurs between the thr and app curves.

For example, (for $n_f = 2$) the first two gates in Fig. 4 (i.e., σ_x and CNOT) implement the transformation for $j = 1$ as

$$|0\rangle_{\rm A}|01\rangle_{\rm F} \to |0\rangle_{\rm A}|11\rangle_{\rm F}, \tag{11}$$

$$|1\rangle_{\rm A}|00\rangle_{\rm F} \to |1\rangle_{\rm A}|11\rangle_{\rm F}. \tag{12}$$

If we attach another CNOT gate (the gate between R_1 and R_3), we obtain the transformation for $j = 3$ as

$$|0\rangle_{\rm A}|11\rangle_{\rm F} \to |0\rangle_{\rm A}|11\rangle_{\rm F}, \tag{13}$$

$$|1\rangle_{\rm A}|00\rangle_{\rm F} \to |1\rangle_{\rm A}|11\rangle_{\rm F}. \tag{14}$$

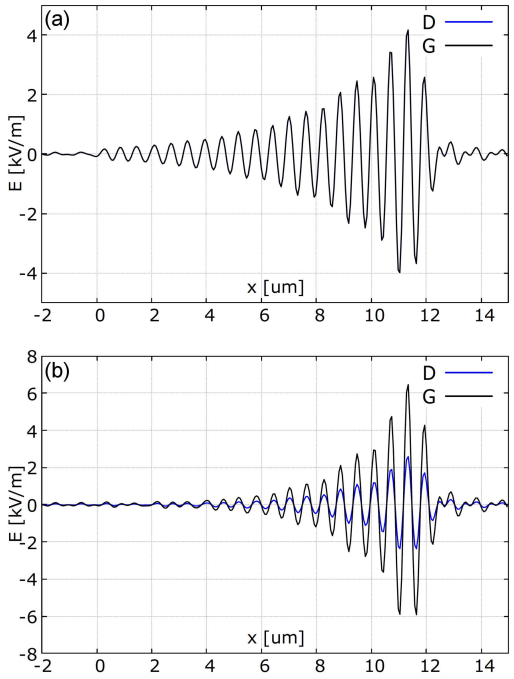

Fig. 7. Electric wave functions of the first (D) and second (G) photon emitted by the atom (located at the point $x_a = 0$). The plots are made (a) for $g_{1n} = g_{2n} = 1.6 \times 10^{-13}$ J/$\sqrt{\text{s}}$ and (b) for $g_{1n} = 1.1 \times 10^{-13}$ J/$\sqrt{\text{s}}$ and $g_{2n} = 2.8 \times 10^{-13}$ J/$\sqrt{\text{s}}$. Values on the horizontal axis are given in μm. The electric field (on the vertical axis) is measured in kV/m. In panel (a), the curve D is not visible because it overlaps with the G curve.

The R_j gates defined by (7)–(8) can be constructed from two standard phase shift gates and R_x gate (as shown in Fig. 5). The standard R_x gate is defined as follows

$$|0\rangle \to \cos\left(\tfrac{\phi}{2}\right)|0\rangle - \mathrm{i}\sin\left(\tfrac{\phi}{2}\right)|1\rangle, \tag{15}$$

$$|1\rangle \to \cos\left(\tfrac{\phi}{2}\right)|1\rangle - \mathrm{i}\sin\left(\tfrac{\phi}{2}\right)|0\rangle. \tag{16}$$

5. Simulation results

The algorithm has been tested in the $n_q = 11$ qubit quantum register. The state of each photon is encoded in the subregister of $n_f = 5$ qubits. The cavity length is equal to $x_{\max} = 3 \times 10^{-5}$ m (the atom position in the cavity is $x_a = 0$) and the time step of the simulation is $\mathrm{d}t = 10^{-17}$ s. We chose a total number of time steps of 4000. The photon levels from $n_{\min} = 32$ to $n_{\max} = 63$ were simulated. We chose the atom excited state energy equal to $E_{\rm A} = 2$ eV. This corresponds to $n = 48$ (48.4029) photon level in the cavity. As the initial state of the system, we chose $|1\rangle_{\rm A}|0\rangle_{\rm F_1}|0\rangle_{\rm F_2}$. The simulation results are shown in Figs. 6–8 and in Table I. Only the results for photons with positive momentum ($k_n > 0$) are presented (the left scheme in Fig. 2).

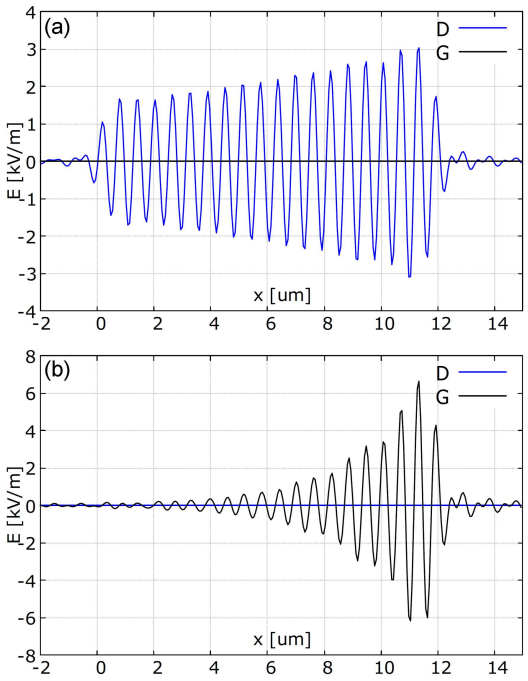

Fig. 8. Electric wave functions of the first (D) and second (G) photon emitted by the atom (located at the point $x_a = 0$) in the case of single-channel decay. The plots are made (a) for $g_{1n} = 1.1 \times 10^{-13}$ J/$\sqrt{\text{s}}$ and $g_{2n} = 0$, and (b) for $g_{1n} = 0$ and $g_{2n} = 2.8 \times 10^{-13}$ J/$\sqrt{\text{s}}$. Values on the horizontal axis are given in μm. The electric field (on the vertical axis) is measured in kV/m.

TABLE I

Decay probabilities for the first and second channel (photon) for different values of the constants g_{1n} and g_{2n} (measured in $\times 10^{-13}$ [J/$\sqrt{\text{s}}$]), $p_{1\text{thr}}$ and $p_{2\text{thr}}$ are the results of theoretical predictions (given in the Appendix by (26), (27) and (19)), while $p_{1\text{sym}}$ and $p_{2\text{sym}}$ are the simulation results.

g_{1n}	g_{2n}	$p_{1\text{thr}}$	$p_{2\text{thr}}$	$p_{1\text{sym}}$	$p_{2\text{sym}}$
2.8	5.04	0.2358	0.7642	0.2361	0.7615
	4.48	0.2809	0.7191	0.2812	0.7171
	3.92	0.3378	0.6622	0.3383	0.6609
	3.36	0.4098	0.5902	0.4104	0.5893
	2.80	0.5000	0.5000	0.5004	0.4992
	2.24	0.6098	0.3902	0.6099	0.3896
	1.68	0.7353	0.2647	0.7348	0.2640
	1.12	0.8621	0.1379	0.8626	0.1379
	0.56	0.9615	0.0385	0.9616	0.0384
	0.28	0.9901	0.0099	0.9900	0.0099

In Fig. 6, in addition to the simulation results, we present the approximation (the least squares method) and the theoretical prediction (given in the Appendix by (23)) of the pA curve.

6. Conclusions

- The evidence from this study suggests that even for the $n_q = 11$ qubits, it is possible to obtain satisfactory results. However, the algorithm is scalable, i.e., an increase in the number of qubits means a higher sampling density of the photon spectrum and, consequently, more accurate results.
- The main advantage of the presented algorithm is lower computational complexity compared to classical algorithms. The number of quantum gates in the UF block (see Fig. 3) is of the order of $\log_2(M)$, where M is the number of modes. This is a much better situation than in the case of classical algorithms, where each mode is simulated separately (the computational complexity is $\mathcal{O}(M)$). In the case of the R block $2M$ phase gates and M R_x-gates (with $\log_2(M)$ control qubits) are needed. The computational complexity of classical interaction algorithm is $\mathcal{O}(M^2)$.
- The number of qubits necessary to perform the simulation is equal to $n_q = N \log_2(M)+1$, where N is the number of simulated photons and M is the number of single photon modes. In the case of classical simulation, the $2NM$ floating point numbers are needed.
- In this work, photons with only positive momentum are simulated. This case does not seem to be physically realistic, however, simulating both positive and negative momentum adds nothing to the matter. The photon emission amplitudes for $+k$ and $-k$ momenta are exactly the same. In the case of two photons and quantum register emulation on a classic computer, we waste 75% of the processor time. A much better solution is to use as many qubits as possible to increase the spectrum density. This improves the quality of the results obtained.
- As is well known, the typical lifetime of the atom excited states is in the order of 10^{-8} s (excluding metastable states). This time is much longer compared to the time of photon propagation in the cavity (on the order of 10^{-14} s). Therefore, we chose g_{in} parameter values corresponding to the deexcitation process time of the order of 10^{-14} s.
- In Fig. 6, there is a discrepancy between pA and thr curves. This is due to the discretization of the photon spectrum. We should obtain the full convergence between both curves for $\mathrm{d}E \to 0$ and $n_f \to \infty$.
- The transition from the momentum representation to the position representation given by the formula (20) in the Appendix is made outside the quantum register.

- As shown in Fig. 7, the shape of the photon wave function generated by i-th decay channel depends only on $\lambda = \lambda_1 + \lambda_2$, not on λ_i.

Appendix

A. Atom–photon interaction

The problem of atom–photon interaction is well known and widely presented in the literature. In this appendix, we present only the most important formulas and conclusions based on [34].

Using dipole approximation, we can write the atom–electromagnetic field interaction coefficients in the following form

$$g_{in} = \langle 0_i, \psi_s | \hat{H}_i | \psi_f, 1_i \rangle \sqrt{-\omega_n} = \frac{e}{m_e} \sqrt{\frac{\hbar^3}{8\epsilon_0 V}}\, \mathrm{e}^{\mathrm{i}\, k_n x_a} \int \mathrm{d}^3\boldsymbol{r}\, \psi_s^*(\boldsymbol{r})\, \boldsymbol{\epsilon} \cdot \nabla \psi_f(\boldsymbol{r}), \tag{17}$$

where $\hat{H}_i$ is the interaction Hamiltonian between the atom and i-th field, $|0\rangle_i$ and $|1\rangle_i$ are the vacuum state and the single-photon state (for mode n), respectively. The initial and final electron wave functions are ψ_s and ψ_f, respectively. The parameter x_a is the position of the atom in the cavity, and V is the volume of the cavity.

The exact solution of the atom deexcitation problem for the case of a single channel decay can be expressed as follows

$$p_A = \exp(-\lambda_i t), \tag{18}$$

where p_A is the probability of finding the atom in the excited state, and

$$\lambda_i = \frac{2\pi |g_{in}|^2}{\hbar\, \mathrm{d}E\, \omega_\mathrm{A}}, \tag{19}$$

where $\mathrm{d}E$ is the distance between the photon energy levels, and E_A ($\omega_\mathrm{A} = E_\mathrm{A}/\hbar$) is the energy (frequency) of the atom excited state (see [34]). The solution (18) is strictly met only in the case of a continuous band of photon energy levels (for $V \to \infty$ and $\mathrm{d}E \to 0$).

The electric field $\boldsymbol{E}$ related to a photon is equal to

$$E(x,t) = -\sqrt{\frac{\hbar}{\epsilon_0 V}} \sum_n \sqrt{2\omega_n} \times \Big[\mathrm{Im}\big(\psi_n(t)\big) \cos(k_n x) + \mathrm{Re}\big(\psi_n(t)\big) \sin(k_n x) \Big]. \tag{20}$$

B. Two-channel decay law

Probability in two-channel decay is

$$p_\mathrm{A} + p_1 + p_2 = 0, \tag{21}$$

where p_A is the probability of finding the atom in the excited state, and p_i is probability of the photon emission in i-th channel.

Decay equations for i-th channel reads as

$$\frac{\mathrm{d}p_i}{p_\mathrm{A}} = \lambda_i\, \mathrm{d}t, \tag{22}$$

where λ_i is the decay constant for i-th channel.

After calculating the differential of (21), then inserting (22) and solving the differential equation (with the initial condition $p_A(0) = 1$), we obtain

$$p_\mathrm{A}(t) = \mathrm{e}^{-(\lambda_1+\lambda_2)t} \tag{23}$$

and

$$p_1(t) = \frac{\lambda_1}{\lambda_1+\lambda_2}\Big(1 - \mathrm{e}^{-(\lambda_1+\lambda_2)t}\Big), \tag{24}$$

$$p_2(t) = \frac{\lambda_2}{\lambda_1+\lambda_2}\Big(1 - \mathrm{e}^{-(\lambda_1+\lambda_2)t}\Big). \tag{25}$$

For $t \to \infty$, we obtain

$$p_1 = \frac{\lambda_1}{\lambda_1+\lambda_2}, \tag{26}$$

$$p_2 = \frac{\lambda_2}{\lambda_1+\lambda_2}. \tag{27}$$

References

[1] R. Feynman, *Int. J. Theor. Phys.* **21**, 467 (1982).

[2] J. Łuczak, B.R. Bułka, *Acta Phys. Pol. A* **133**, 748 (2018).

[3] T. Maciażek, *Acta Phys. Pol. A* **136**, 824 (2019).

[4] P.W. Shor, in: *Proc. 35th Annual Symposium on Foundations of Computer Science, Santa Fe (NM) 1994*, IEEE, 1994, p. 124.

[5] L.K. Grover, *Am. J. Phys.* **69**, 769 (2001).

[6] Min-Ho Lee, Nark Nyul Choi, G. Tanner, *Acta Phys. Pol. A* **140**, 538 (2021).

[7] S. Lloyd, *Science* **273**, 1073 (1996).

[8] T. Schaetz, C.R. Monroe, T. Esslinger, *New J. Phys.* **15**, 085009 (2013).

[9] B.P. Lanyon, C. Hempel, D. Nigg et al., *Science* **334**, 57 (2011).

[10] A.M. Childs, D. Maslov, Y. Nam, N.J. Ross, Y. Su, *PNAS* **115**, 9456 (2018).

[11] D. Wecker, M.B. Hastings, N. Wiebe, B.K. Clark, C. Nayak, M. Troyer, *Phys. Rev. A* **92**, 062318 (2015).

[12] C. Kokail, C. Maier, R. van Bijnen et al., *Nature* **569**, (2019).

[13] D. Wecker, B. Bauer, B.K. Clark, M.B. Hastings, M. Troyer, *Phys. Rev. A* **90**, 022305, (2014).

[14] C. Hempel, C. Maier, J. Romero et al., *Phys. Rev. X* **8**, 031022 (2018).

[15] S.P. Jordan, K.S.M. Lee, J. Preskill, *Science* **336**, 1130 (2012).

[16] S. Wiesner, arXiv:quant-ph/9603028, 1996.

[17] C. Zalka, *Fortschr. Phys.* **46**, 877-879 (1998).

[18] G. Strini, *Fortschr. Phys.* **50**, 171 (2002).

[19] G. Benenti, G. Strini, *Am. J. Phys.* **76**, 657 (2008).

[20] M. Ostrowski, *Acta Phys. Pol. A* **137**, (2020).

[21] M. Ostrowski, *Bull. Pol. Acad. Tech.* **68**, (2020).

[22] M. Ostrowski, *Przegląd. Elektrotechniczny* **10**, 167 (2020).

[23] Ch. Anastopoulos, *Int. J. Theor. Phys.***58**, 890 (2019).

[24] S. Vaintraub, K. Blaum, M. Hass, O. Heber, O. Aviv, M. Rappaport, A. Dhal, I. Mador, A. Wolf, arXiv:1402.3978, 2014.

[25] V. Buzek, G. Drobny, M.G. Kim, M. Havukainen, P.L. Knight, *Phys. Rev. A* **60**, 582 (1999).

[26] N.P. Bauman, G.H. Low, K. Kowalski, *J. Chem. Phys.* **151**, 234114 (2019).

[27] A. Kumar, A. Asthana, C. Masteran, E.F. Valeev, Y. Zhang, L. Cincio, S. Tretiak, P.A. Dub, arXiv:2201.09852, 2022.

[28] O. Higgott, D. Wang, S. Brierley, arXiv:1805.08138, 2019.

[29] H. Taniyama, H. Sumikura, M. Notomi, *Opt. Express* **27**, 12070 (2019).

[30] M. Bindhani, B.K. Behera, P.K. Panigrahi, "Quantum Simulation of Jaynes-Cummings Model on IBM Q System" (2020).

[31] Qiskit.

[32] A.M. Childs, Y. Su, M.C. Tran, N. Wiebe, S. Zhu, *Phys. Rev. X* **11**, 011020 (2021).

[33] Wikipedia, Gray code.

[34] H. Haken *Light: Waves, Photons, Atoms*, North-Holland, 1985.